Advanced Practices in Aerospace and Energy Engineering - Research Article

Advances in Mechanical Engineering

Advances in Mechanical Engineering
2021, Vol. 13(11) 1–9

DOI: 10.1177/16878140211065147
journals.sagepub.com/home/ade
SAGE

Non-isothermal rarefied gas flow in microtube with constant wall temperature

Iva Guranov, Snežana Milićev and Nevena Stevanović

Abstract

In this paper, pressure-driven gas flow through a microtube with constant wall temperature is considered. The ratio of the molecular mean free path and the diameter of the microtube cannot be negligible. Therefore, the gas rarefaction is taken into account. A solution is obtained for subsonic as well as slip and continuum gas flow. Velocity, pressure, and temperature fields are analytically attained by macroscopic approach, using continuity, Navier-Stokes, and energy equations, with the first order boundary conditions for velocity and temperature. Characteristic variables are expressed in the form of perturbation series. The first approximation stands for solution to the continuum flow. The second one reveals the effects of gas rarefaction, inertia, and dissipation. Solutions for compressible and incompressible gas flow are presented and compared with the available results from the literature. A good matching has been achieved. This enables using proposed method for solving other microtube gas flows, which are common in various fields of engineering, biomedicine, pharmacy, etc. The main contribution of this paper is the integral treatment of several important effects such as rarefaction, compressibility, temperature field variability, inertia, and viscous dissipation in the presented solutions. Since the solutions are analytical, they are useful and easily applicable.

Keywords

Microtube, rarefied gas, slip flow, constant wall temperature, analytical solution

Date received: 24 July 2021; accepted: 16 November 2021

Handling Editor: Ms. Chenhui Liang

Introduction

Microelectromechanical systems (MEMS) are small-sized devices consisted of mechanical and electro components, which play a significant role in electromagnetic, thermal, pneumatic, and many other fields.[1] MEMS's characteristical dimension takes the values between 1 μm and 1 mm. As all systems recognizable to humans can be classified as astronomical, macro (human size), and microscales, MEMS belong to microscale systems. Surface and volume effects have different influence in these scales. In case of microscale gas flow, surface forces are significantly more influential than volume ones.

In gas flow through microtube, the ratio of the molecular mean free path $\tilde{\lambda}$ and microtube diameter $\tilde{D}$, which represents Knudsen number, is not negligible. According to values of Knudsen number, which is the measure of rarefaction, characteristic regimes are: continuum flow ($\mathrm{Kn} \leqslant 0.001$), slip flow ($0.001 \leqslant \mathrm{Kn} \leqslant 0.1$), transition regime ($0.1 \leqslant \mathrm{Kn} \leqslant 10$), and free molecular flow ($\mathrm{Kn} > 10$).[2]

Microtubes are frequently used as components of MEMS. They can be transparent, flexible, and biocompatible, which makes them suitable for use in

Faculty of Mechanical Engineering, University of Belgrade, Belgrade, Serbia

Corresponding author:
Iva Guranov, Faculty of Mechanical Engineering, University of Belgrade, Kraljice Marije 16, Belgrade 11000, Serbia.
Email: iguranov@mas.bg.ac.rs

biomedicine. Microtubes are often essential parts of actuators, sensors, valves, etc. Moreover, they are an integral part of micro heat exchangers. They are used, primarily as cooling devices, in many fields: automotive, aerospace, power and process industries, thermotechnics, microelectronics, bioengineering, etc. Non-isothermal gas flow in microtubes under various temperature conditions is present in all mentioned fields and devices. That is why finding solutions for gas flow, for different geometries and different temperature boundary conditions, are very significant.

The problem of the rarefied gas flow in a microtube with constant cross section has been considered by various authors. Sharipov and Seleznev[3] analyzed pressure-driven isothermal rarefied gas flow between two reservoirs connected with microtube. The authors solved the problem for all Knudsen numbers by kinetic theory of gases. The problem of isothermal rarefied slip gas flow in microtubes, which is considered as compressible, axisymmetric, and at low Reynolds numbers is considered in Radenković et al.[4] The analytical solution was reached by macroscopic approach with Maxwell slip boundary condition. Hemadri et al.[5] presented an experimental study of rarefied gas flow with heat transfer in circular tube with constant wall temperature. There, for the first time, the local temperature measurements were performed in rarefied gas flow in order to analyze Nusselt number values. Xiao et al.[6] gave solution obtained by solving momentum and energy equation, with second order velocity slip and temperature jump boundary conditions, combined with isoflux condition at the surface of the microtube. An analytical solution for temperature field and Nusselt number, for hydrodynamically and thermally fully developed gas flow, is obtained by neglecting compressibility, viscous dissipation, and axial conduction. Spiga and Vocale[7] considered steady fully-developed slip gas flow in elliptic microducts with axial uniform heat flux, neglecting compressibility and viscous dissipation, numerically, by a commercial software. A similar analysis is performed by Kushwaha and Sahu[8] taking into account viscous dissipation.

Several authors examined extended Graetz problem of rarefied gas flow in microtube.[9–11] Barisik et al.[9] solved problem analytically, comprising axial conduction and viscous dissipation effects, using Gram-Schmidt orthogonalization technique. Comparative analysis between first and second order slip model of incompressible gas flow, with viscous dissipation and axial heat conduction taken into account, is presented by Aziz and Niedbalski,[10] with combining analytical and numerical approach. Chen[11] researched slip flow with heat transfer in microtubes based on lattice Boltzmann model.

The fully-developed temperature profile and Nusselt value are analytically determined for incompressible rarefied gas flow in a microtube, with second order velocity slip and temperature jump boundary conditions and constant wall heat flux.[12] The solution includes viscous dissipation as well as axial conduction effect. In Maharjan et al.[13] and Valougeorgis and Pantazis,[14] authors considered heat transfer of rarefied gas flow between two coaxial cylinders at different temperatures. In Maharjan et al.[13] solution is obtained by S-model kinetic equation and DSMC technique, with implemented Lin and Willis temperature jump boundary condition. Valougeorgis and Pantazis[14] solution is based on the nonlinear S kinetic model with Cercignani–Lampis boundary conditions. Colin[15] wrote review on convective heat transfer in microgeometries with focus on rarefaction effects in slip flow regime. In that review, various heat transfer conditions (constant wall temperature, constant heat flux) and various microgeometries (circular, parallel plate, rectangular, trapezoidal or triangular microchannel, microtube with annular or semi-circular cross section), with influence of specific effects (viscous dissipation, axial conduction, variable fluid properties), are examined.

In this paper, stationary axisymmetric rarefied pressure-driven slip gas flow in microtube with constant wall temperature is analyzed. The solution is obtained for subsonic gas flow with moderately high Reynolds numbers, that is inertia effect is included. Solution procedure is based on assuming all variables by perturbation series. An analytical solution for velocity, pressure and temperature are presented for both compressible and incompressible gas flow.

Governing equations and problem description

System of governing equations (energy equation, momentum equation projected on longitudinal direction, momentum equation projected on radial direction, continuity equation, equation of state of an ideal gas)[1] with Maxwell[16] velocity slip and Smoluchowski von Smolan[17] temperature jump boundary conditions in cylindrical coordinates are respectively:

$$\begin{aligned}\tilde{\rho}\tilde{c}_p\left(\tilde{v}\frac{\partial\tilde{T}}{\partial\tilde{r}}+\tilde{u}\frac{\partial\tilde{T}}{\partial\tilde{z}}\right) &= \frac{1}{\tilde{r}}\frac{\partial}{\partial\tilde{r}}\left(\tilde{k}\tilde{r}\frac{\partial\tilde{T}}{\partial\tilde{r}}\right)+\frac{\partial}{\partial\tilde{z}}\left(\tilde{k}\frac{\partial\tilde{T}}{\partial\tilde{z}}\right)\\ &+\tilde{v}\frac{\partial\tilde{p}}{\partial\tilde{r}}+\tilde{u}\frac{\partial\tilde{p}}{\partial\tilde{z}}+\\ &+2\tilde{\mu}\left(\left(\frac{\partial\tilde{v}}{\partial\tilde{r}}\right)^2+\left(\frac{\partial\tilde{u}}{\partial\tilde{z}}\right)^2+\left(\frac{\tilde{v}}{\tilde{r}}\right)^2\right)+\tilde{\mu}\left(\frac{\partial\tilde{u}}{\partial\tilde{r}}+\frac{\partial\tilde{v}}{\partial\tilde{z}}\right)^2\\ &-\frac{2}{3}\tilde{\mu}\left(\frac{1}{\tilde{r}}\frac{\partial(\tilde{r}\tilde{v})}{\partial\tilde{r}}+\frac{\partial\tilde{u}}{\partial\tilde{z}}\right)^2\end{aligned} \tag{1}$$

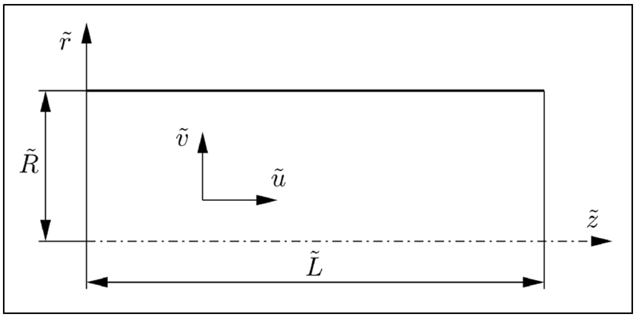

Figure 1. Microtube geometry.

$$\tilde{\rho}\left(\tilde{v}\frac{\partial\tilde{u}}{\partial\tilde{r}}+\tilde{u}\frac{\partial\tilde{u}}{\partial\tilde{z}}\right)=\tilde{\mu}\left(\frac{\partial^2\tilde{u}}{\partial\tilde{r}^2}+\frac{\partial^2\tilde{v}}{\partial\tilde{r}\partial\tilde{z}}\right)-\frac{\partial\tilde{p}}{\partial\tilde{z}}-\frac{2}{3}\tilde{\mu}\left(\frac{\partial}{\partial\tilde{z}}\frac{1}{\tilde{r}}\frac{\partial(\tilde{r}\tilde{v})}{\partial\tilde{r}}\right)+\frac{4}{3}\tilde{\mu}\frac{\partial^2\tilde{u}}{\partial\tilde{z}^2}+\frac{\tilde{\mu}}{\tilde{r}}\left(\frac{\partial\tilde{u}}{\partial\tilde{r}}+\frac{\partial\tilde{v}}{\partial\tilde{z}}\right) \quad (2)$$

$$\tilde{\rho}\left(\tilde{v}\frac{\partial\tilde{v}}{\partial\tilde{r}}+\tilde{u}\frac{\partial\tilde{v}}{\partial\tilde{z}}\right)=-\frac{\partial\tilde{p}}{\partial\tilde{r}}+2\tilde{\mu}\frac{\partial^2\tilde{v}}{\partial\tilde{r}^2}-\frac{2}{3}\tilde{\mu}\left(\frac{\partial}{\partial\tilde{r}}\left(\frac{1}{\tilde{r}}\frac{\partial(\tilde{r}\tilde{v})}{\partial\tilde{r}}\right)+\frac{\partial^2\tilde{u}}{\partial\tilde{r}\partial\tilde{z}}\right)+\tilde{\mu}\left(\frac{\partial^2\tilde{u}}{\partial\tilde{r}\partial\tilde{z}}+\frac{\partial^2\tilde{v}}{\partial\tilde{z}^2}\right)+2\frac{\tilde{\mu}}{\tilde{r}}\frac{\partial\tilde{v}}{\partial\tilde{r}}-\tilde{\mu}\frac{\tilde{v}}{\tilde{r}^2} \quad (3)$$

$$\frac{1}{\tilde{r}}\frac{\partial(\tilde{\rho}\tilde{r}\tilde{v})}{\partial\tilde{r}}+\frac{\partial(\tilde{\rho}\tilde{u})}{\partial\tilde{z}}=0 \quad (4)$$

$$\tilde{p}=\tilde{\rho}\tilde{R}_g\tilde{T} \quad (5)$$

$$\tilde{u}|_{\tilde{r}=\tilde{R}}=-\frac{2-\sigma_v}{\sigma_v}\tilde{\lambda}\frac{\partial\tilde{u}}{\partial\tilde{r}}\bigg|_{\tilde{r}=\tilde{R}} \quad (6)$$

$$\tilde{T}\big|_{\tilde{r}=\tilde{R}}=\tilde{T}_w-\frac{2-\sigma_T}{\sigma_T}\frac{2\kappa}{\kappa+1}\frac{\tilde{\lambda}}{\mathrm{Pr}}\frac{\partial\tilde{T}}{\partial\tilde{r}}\bigg|_{\tilde{r}=\tilde{R}} \quad (7)$$

where $\tilde{u}$, $\tilde{v}$, $\tilde{p}$, $\tilde{T}$, $\tilde{\rho}$, $\tilde{r}$, $\tilde{z}$ are respectively longitudinal velocity (m/s), radial velocity (m/s), pressure (Pa), temperature (K), density (kg/m^3), radial and longitudinal coordinate (m) (Figure 1). σ_v (–) and σ_T (–) are momentum and thermal accommodation coefficients, $\tilde{c}_p$ is specific heat coefficient at constant pressure (J/(kg K)), $\tilde{R}_g$ specific gas constant (J/(kg K)), $\tilde{R}$ radius of microtube (m), $\tilde{T}_w$ the microtube wall temperature (K), κ heat capacity ratio (–).

System of governing equations and boundary conditions (1)–(7) is transformed in non-dimensional form by defining non-dimensional variables:

$$u=\frac{\tilde{u}}{\tilde{u}_r},v=\frac{\tilde{v}}{\tilde{u}_r},p=\frac{\tilde{p}}{\tilde{p}_r},T=\frac{\tilde{T}}{\tilde{T}_w},\rho=\frac{\tilde{\rho}}{\tilde{\rho}_r},\quad r=\frac{\tilde{r}}{\tilde{R}},z=\frac{\tilde{z}}{\tilde{L}},\mu=\frac{\tilde{\mu}}{\tilde{\mu}_r},k=\frac{\tilde{k}}{\tilde{k}_r}, \quad (8)$$

where $\tilde{u}_r$ is mean longitudinal velocity at the exit cross section, $\tilde{p}_r$ pressure at the exit cross section, $\tilde{\rho}_r$ reference density ($\tilde{\rho}_r=\tilde{p}_r/(\tilde{R}_g\tilde{T}_w)$), $\tilde{L}$ microtube length (m), $\tilde{\mu}_r$ reference dynamic viscosity, and $\tilde{k}_r$ thermal conductivity, both defined for $\tilde{T}_w$.

Dimensionless equations are simplified by the following assumptions:

- small parameter ε ($\varepsilon << 1$) is defined as

$$\varepsilon=\frac{2\tilde{R}}{\tilde{L}} \quad (9)$$

- radial velocity component is much smaller than longitudinal velocity component

$$\tilde{v}=\varepsilon\tilde{V},\quad \tilde{V}=O(1) \quad (10)$$

- subsonic gas flow

$$\kappa\mathrm{Ma}_\mathrm{r}^2=\gamma\varepsilon^m,\quad \gamma=O(1),\quad m>0, \quad (11)$$

where reference Mach number is $\mathrm{Ma_r}=\tilde{u}_r/\sqrt{\kappa\tilde{p}_r/\tilde{\rho}_r}$;

- slip gas flow

$$\mathrm{Kn_r}=\eta\varepsilon^n,\quad \eta=O(1),\quad n>0, \quad (12)$$

where $\mathrm{Kn_r}=\tilde{\lambda}_r/2\tilde{R}$ is reference Knudsen number;

- low value of Mach number allows following correlation

$$\frac{\kappa\mathrm{Ma}_\mathrm{r}^2}{\mathrm{Re_r}}=\beta\varepsilon,\quad \beta=O(1) \quad (13)$$

in which $\mathrm{Re_r}=\tilde{\rho}_r\tilde{u}_r2\tilde{R}/\tilde{\mu}_r$ is reference Reynolds number.

From definition of reference Mach, Knudsen, and Reynolds number, relationship between these numbers is:

$$\mathrm{Kn_r}=\sqrt{\frac{\pi\kappa}{2}}\frac{\mathrm{Ma_r}}{\mathrm{Re_r}} \quad (14)$$

Also, from equations (11) and (13) reference Reynolds number follows:

$$\mathrm{Re_r}=\gamma\varepsilon^{m-1}/\beta, \quad (15)$$

where value of parameter m determines the order of magnitude of reference Reynolds number (low or moderately high Reynolds number). Involving equations (11), (12), (15) into equation (14) relationship between parameters γ, η, and β is obtained:

$$\gamma=\frac{\beta^2\pi}{2\eta^2} \quad (16)$$

Parameters γ, η, β, m, and n are introduced in order to make the model more flexible, so that it provides a wider application. Without these parameters introduced in equations (11)–(13), for a certain value of small parameter ε, which represents ratio of microtube diameter and its length, there would be only one corresponding value for Mach, Knudsen, and Reynolds number. By bringing in parameters γ, η, β, m, and n into the model, for a certain value of small parameter ε, results could be obtained for a wide range of Mach and Knudsen number values within subsonic and slip flow regime, that is corresponding wide range of Reynolds number values. Furthermore, considering equation (15) together with relation $2n + m = 2$, which is obtained from assumptions (11), (12) and equations (14)–(16), leads to the solution for two characteristic regimes[18]:

$$\begin{aligned}&\text{small Reynolds numbers:}\\ &\mathrm{Re_r}<1: \quad 1<m<2, \quad 0<n<1/2\end{aligned} \tag{17}$$

$$\begin{aligned}&\text{moderately high Reynolds numbers:}\\ &\mathrm{Re_r}\geqslant 1: \quad 0<m\leqslant 1, \quad 1/2\leqslant n<1\end{aligned} \tag{18}$$

Prandtl number has the same value in the whole flow field:

$$\mathrm{Pr} = \mathrm{Pr_r} = \tilde{c}_p \frac{\tilde{\mu}_r}{\tilde{k}_r} \tag{19}$$

Dimensionless form of governing equations

Considering previous assumptions, dimensionless system of governing equations and boundary conditions follows:

$$\begin{aligned}&\mathrm{Pr}\frac{\gamma\varepsilon^m}{2\beta}\rho V\frac{\partial T}{\partial r} + \mathrm{Pr}\frac{\gamma\varepsilon^m}{4\beta}\rho u\frac{\partial T}{\partial z} = \frac{1}{r}\frac{\partial}{\partial r}\left(kr\frac{\partial T}{\partial r}\right)\\ &+ \mathrm{Pr}\frac{\kappa-1}{4\kappa}\frac{\gamma\varepsilon^m}{\beta}u\frac{\partial p}{\partial z} + \mu\mathrm{Pr}(\kappa-1)\frac{\gamma\varepsilon^m}{\kappa}\left(\frac{\partial u}{\partial r}\right)^2\end{aligned} \tag{20}$$

$$2\gamma\varepsilon^m\rho V\frac{\partial u}{\partial r} + \gamma\varepsilon^m\rho u\frac{\partial u}{\partial z} = -\frac{\partial p}{\partial z} + 4\beta\mu\frac{\partial^2 u}{\partial r^2} + 4\beta\frac{\mu}{r}\frac{\partial u}{\partial r} \tag{21}$$

$$\frac{\partial p}{\partial r} = 0 \tag{22}$$

$$\frac{2}{r}\frac{\partial(\rho r V)}{\partial r} + \frac{\partial(\rho u)}{\partial z} = 0 \tag{23}$$

$$p = \rho T \tag{24}$$

$$u|_{r=1} = -\frac{2-\sigma_v}{\sigma_v}2\mathrm{Kn_r}\frac{T^{a+0.5}}{p}\frac{\partial u}{\partial r}\bigg|_{r=1} \tag{25}$$

$$T|_{r=1} = 1 - \frac{2-\sigma_T}{\sigma_T}\frac{4\kappa}{\kappa+1}\frac{\mathrm{Kn_r}}{\mathrm{Pr}}\frac{T^{a+0.5}}{p}\frac{\partial T}{\partial r}\bigg|_{r=1} \tag{26}$$

According to molecular model of solid spheres, dimensionless values of dynamic viscosity and thermal conductivity were assumed as $\mu = k = T^a$, where values of viscosity-temperature parameter a may cover different models. Parameter a with value $a = 0.5$ represents model of elastic molecules, $a = 1$ represents model of Maxwell molecules, while $a = 0$ covers the case of constant viscosity and thermal conductivity $\mu = k = 1$.

In order to solve system of equations with perturbation approach, all characteristic dimensionless variables (u, v, p, ρ, T) are expressed in form of perturbation series[19]:

$$f = f_0 + \mathrm{Kn_r}f_1 + O(\mathrm{Kn_r^2}) \tag{27}$$

This assumption of perturbation series in power of Knudsen number, equation (27), assures the rarefaction effect to appear in the second approximation. With the intent to achieve the same order of magnitude for slip, as well as inertia and dissipation effects, that is to make sure that all these effects appear in the second approximation, values for parameters m and n have to be $m = n = 2/3$. This follows from equations (20), (21) and its correlation $2n + m = 2$. Thus, such flow corresponds to moderately high values Reynolds number regime, equation (18). Now, from system of governing equations and boundary conditions (20)–(26), two approximations follow. The first approximation corresponds to continuum flow (variables marked with index "0") while the second approximation comprises influence of slip, inertia, and dissipation (variables marked with "1").

- The governing equations and boundary conditions $O(1)$ are:

$$0 = \frac{1}{r}\frac{\partial}{\partial r}\left(rT_0^a\frac{\partial T_0}{\partial r}\right) \tag{28}$$

$$\frac{\partial p_0}{\partial z} = 4\beta T_0^a\frac{\partial^2 u_0}{\partial r^2} + \frac{4\beta}{r}T_0^a\frac{\partial u_0}{\partial r} \tag{29}$$

$$\frac{\partial p_0}{\partial r} = 0 \tag{30}$$

$$\int_0^1 2\rho_0 u_0 r\mathrm{d}r = \dot{m}_0 \tag{31}$$

$$\frac{\partial T_0}{\partial r}\bigg|_{r=0} = 0, T_0|_{r=1} = 1 \tag{32}$$

$$\frac{\partial u_0}{\partial r}\bigg|_{r=0} = 0, u_0|_{r=1} = 0 \tag{33}$$

$$p_0|_{z=1} = 1 \tag{34}$$

- The governing equations and boundary conditions $O(\mathrm{Kn_r})$ are:

$$\frac{\Pr}{2}\frac{\gamma}{\beta}\rho_0 V_0 \frac{\partial T_0}{\partial r} + \frac{\Pr}{4}\frac{\gamma}{\beta}\rho_0 u_0 \frac{\partial T_0}{\partial z} = \eta \frac{1}{r}\frac{\partial}{\partial r}\left(r\left(T_0^a \frac{\partial T_1}{\partial r} + aT_1 T_0^{a-1}\frac{\partial T_0}{\partial r}\right)\right) + + \Pr\frac{\gamma}{\beta}\frac{\kappa-1}{4\kappa}u_0\frac{\partial p_0}{\partial z} + \Pr\frac{\gamma}{\kappa}(\kappa-1)T_0^a\left(\frac{\partial u_0}{\partial r}\right)^2 \tag{35}$$

$$\frac{2\gamma}{\eta}\rho_0 V_0 \frac{\partial u_0}{\partial r} + \frac{\gamma}{\eta}\rho_0 u_0 \frac{\partial u_0}{\partial z} + \frac{\partial p_1}{\partial z} = 4\beta T_0^a \frac{\partial^2 u_1}{\partial r^2} + 4\beta a T_0^{a-1} T_1 \frac{\partial^2 u_0}{\partial r^2} + \frac{4\beta}{r}T_0^a \frac{\partial u_1}{\partial r} + + \frac{4\beta}{r} a T_0^{a-1} T_1 \frac{\partial u_0}{\partial r} \tag{36}$$

$$\frac{\partial p_1}{\partial r} = 0 \tag{37}$$

$$\int_0^1 2(\rho_0 u_1 + \rho_1 u_0)\, r\mathrm{d}r = \dot{m}_1 \tag{38}$$

$$\left.\frac{\partial T_1}{\partial r}\right|_{r=0} = 0, T_1|_{r=1} = -\frac{2-\sigma_T}{\sigma_T}\frac{4\kappa}{\kappa+1}\frac{1}{\Pr}\frac{{T_0}^{a+0.5}}{p_0}\left.\frac{\partial T_0}{\partial r}\right|_{r=1} \tag{39}$$

$$\left.\frac{\partial u_1}{\partial r}\right|_{r=0} = 0, u_1|_{r=1} = -\frac{2-\sigma_v}{\sigma_v}2\frac{{T_0}^{a+0.5}}{p_0}\left.\frac{\partial u_0}{\partial r}\right|_{r=1} \tag{40}$$

$$p_1|_{z=1} = 0 \tag{41}$$

For defined mass flow in microtube, the whole value of $\dot{m}$ is in the first approximation, so $\dot{m}_0 = 1$ and $\dot{m}_1 = 0$.

The solution procedure goes for both approximations in following way. Firstly, energy equations for both approximations (28), (35) are solved with appropriate axisymmetric and boundary conditions (32), (39). Attained solution for temperature field is:

$$T = T_0 + \mathrm{Kn_r}T_1 = 1 + \mathrm{Kn_r^2 Re_r^2}\frac{(1-\kappa)}{256\pi\beta^2\kappa}{p_0'}^2\Pr\left(r^2-1\right)^2 \tag{42}$$

Secondly, the longitudinal velocity follows from the momentum equations (29), (36), with axisymmetric and boundary conditions (33), (40):

$$u = u_0 + \mathrm{Kn_r}u_1 = \frac{p_0'}{16\beta}\left(r^2-1\right) + \mathrm{Kn_r}\left[-\frac{2-\sigma_v}{\sigma_v}\frac{p_0'}{4\beta p_0} + \frac{p_1'}{16\beta}\left(r^2-1\right) + \frac{\mathrm{Kn_r Re_r^2}}{2048\pi\beta^3}\left(\rho_0 p_0' p_0'' + \frac{a\Pr(\kappa-1){p_0'}^3}{2\kappa}\right)\left(\frac{r^6}{9}-\frac{r^4}{2}+r^2-\frac{11}{18}\right)\right] \tag{43}$$

Solution for the pressure field is derived from integral form of continuity equations (31), (38).

Regarding compressibility effect, this paper examines two cases: compressible and incompressible microtube gas flow.

Solution for compressible gas flow

From dimensionless equation of state of an ideal gas (24), assuming density, pressure and temperature by perturbation series (27), with obtained solution $T_0 = 1$, first and second order approximation of density are: $\rho_0 = p_0$ and $\rho_1 = p_1 - p_0 T_1$. Then, from continuity equations (31) and (38), for known pressure at the exit (34), (41), the solution for pressure distribution in compressible microtube gas flow follows:

$$p = p_0 + \mathrm{Kn_r}p_1 = p_0 + \mathrm{Kn_r}\left[\frac{2-\sigma_v}{\sigma_v}8\left(\frac{1}{p_0}-1\right) + 2\mathrm{Kn_r Re_r^2}\frac{\ln p_0}{\pi p_0}\left(2-(1+a)\Pr\frac{\kappa-1}{\kappa}\right)\right] \tag{44}$$

Here, the first approximation of pressure is:

$$p_0 = \sqrt{1+64\beta(1-z)} \tag{45}$$

According to this pressure solution, from general solutions for temperature (42) and velocity (43), temperature and velocity distributions for compressible gas flow in microtube are, respectively:

$$T = T_0 + \mathrm{Kn_r}T_1 = 1 + 4\mathrm{Kn_r^2 Re_r^2}\Pr\frac{(1-\kappa)}{\pi\kappa p_0^2}\left(r^2-1\right)^2 \tag{46}$$

$$u = u_0 + \mathrm{Kn_r}u_1 = \frac{2}{p_0}\left(1-r^2\right) + + \mathrm{Kn_r}\left[\frac{2-\sigma_v}{\sigma_v}\frac{8}{p_0^2} + \frac{p_1'}{16\beta}\left(r^2-1\right) + \mathrm{Kn_r Re_r^2}\frac{8}{\pi p_0^3}\left(2-\frac{a\Pr(\kappa-1)}{\kappa}\right)\left(\frac{r^6}{9}-\frac{r^4}{2}+r^2-\frac{11}{18}\right)\right] \tag{47}$$

Solution for incompressible gas flow

For incompressible gas flow, complete density is contained in the first approximation: $\rho_0 = 1$, while $\rho_1 = 0$. Now, by integrating continuity equations (31) and (38), for known pressure at the exit (34) and (41), the pressure distribution for incompressible microtube gas flow follows:

$$p = p_0 + \mathrm{Kn_r}p_1 = p_0 + \mathrm{Kn_r}\left[-\frac{2-\sigma_v}{\sigma_v}8\ln p_0 + 2a\mathrm{Kn_r Re_r^2}\Pr\frac{\kappa-1}{\pi\kappa}(1-p_0)\right] \tag{48}$$

Here, the first pressure approximation is:

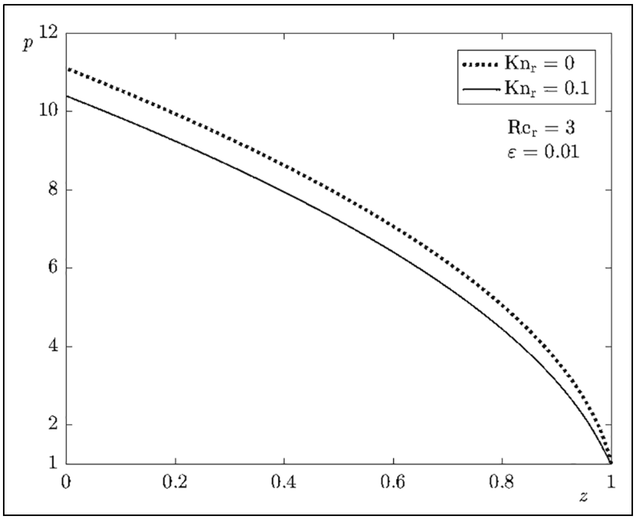

Figure 2. The pressure distribution in microtube for compressible gas flow (44), for continuum ($\mathrm{Kn_r} = 0$) and slip ($\mathrm{Kn_r} = 0.1$).

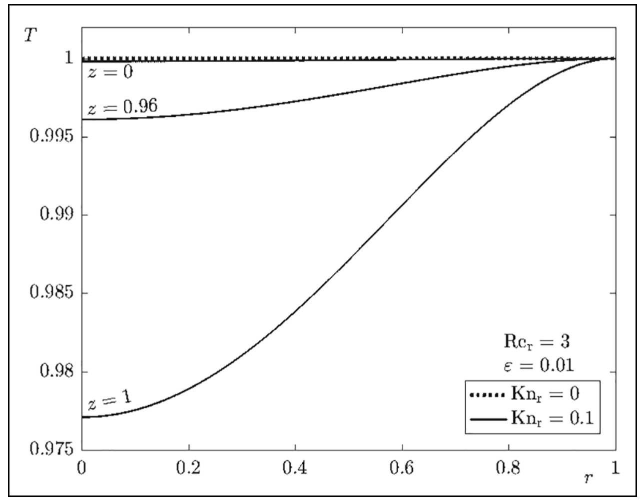

Figure 3. The temperature profile (46) at different cross sections of microtube for compressible gas flow, for continuum ($\mathrm{Kn_r} = 0$) and slip ($\mathrm{Kn_r} = 0.1$).

$$p_0 = 32\beta(1 - z) + 1 \tag{49}$$

Finally, general solution for temperature (42) and velocity (43), with the first pressure approximation (49) provide results for incompressible gas flow in microtube:

$$T = T_0 + \mathrm{Kn_r} T_1 = 1 + 4\mathrm{Kn_r^2}\mathrm{Re_r^2}\mathrm{Pr}\frac{(1-\kappa)}{\pi\kappa}\left(r^2 - 1\right)^2 \tag{50}$$

$$\begin{aligned} u = u_0 + \mathrm{Kn_r} u_1 &= 2\left(1 - r^2\right) + \\ &+ \mathrm{Kn_r}\left[\frac{2-\sigma_v}{\sigma_v}\frac{8}{p_0} + \frac{p_1{}'}{16\beta}\left(r^2 - 1\right)\right. \\ &\left. -8a\mathrm{Kn_r}\mathrm{Re_r^2}\mathrm{Pr}\frac{\kappa - 1}{\pi\kappa}\left(\frac{r^6}{9} - \frac{r^4}{2} + r^2 - \frac{11}{18}\right)\right] \end{aligned} \tag{51}$$

Results and discussion

All presented results are obtained for diatomic gas $\kappa = 1.4$, $\mathrm{Pr} = 0.7$, for diffuse reflection $\sigma_v = 1$ and the perfect energy exchange $\sigma_T = 1$. Beside this, for obtaining pressure, temperature and velocity in microtube, the three dimensionless parameters are necessary and sufficient. Here, for the results presentation, Reynolds number, Knudsen number, and small parameter ε are chosen.

The pressure, temperature, and velocity distribution for compressible rarefied gas flow in microtube with constant wall temperature, for the regime with moderately high Reynolds number, are presented in Figures 2 to 4.

The influence of Knudsen number on pressure distribution along the microtube is presented in Figure 2. It is evident that for the same Reynolds number at the exit cross section of microtube and for the same microtube geometry, increase of rarefaction, that is, of the reference Knudsen number leads to the lower pressure in the microtube. This means that for the same flow conditions at the exit, pressure along the microtube is lower when rarefaction is taken into account.

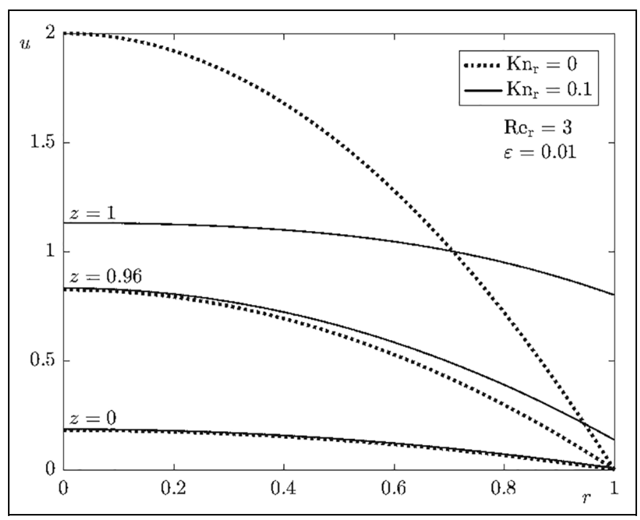

Figure 4. The velocity profile (47) at different cross sections of microtube for compressible gas flow, for continuum ($\mathrm{Kn_r} = 0$) and slip ($\mathrm{Kn_r} = 0.1$).

The temperature and velocity profiles at different cross sections of microtube, $z = 0$, $z = 0.96$, and $z = 1$, for continuum ($\mathrm{Kn_r} = 0$) and slip gas flow ($\mathrm{Kn_r} = 0.1$), are presented in Figures 3 and 4, respectively. The presented model (46) shows that the flow appears to be isothermal for continuum flow conditions, $\mathrm{Kn_r} = 0$ (Figure 3). Furthermore, the rarefaction leads to the temperature change in the cross section as well as along

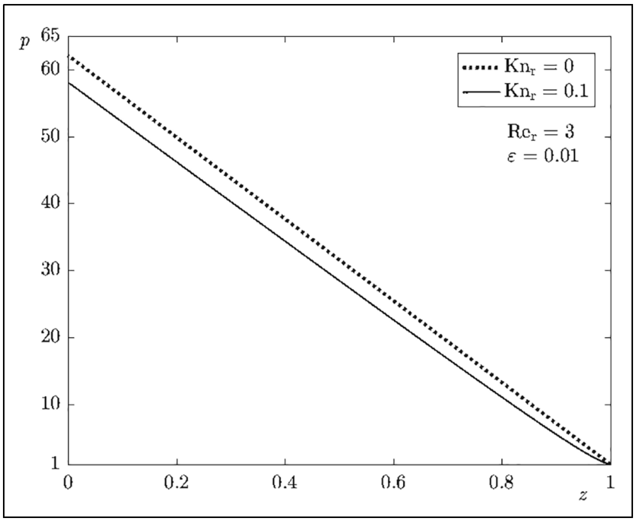

Figure 5. The pressure distribution in microtube for incompressible gas flow (54), for continuum ($\mathrm{Kn_r}=0$) and slip ($\mathrm{Kn_r}=0.1$).

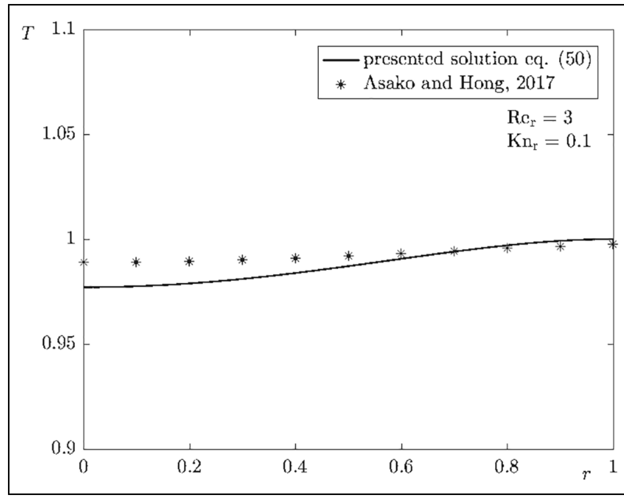

Figure 6. Temperature profile for incompressible gas flow.

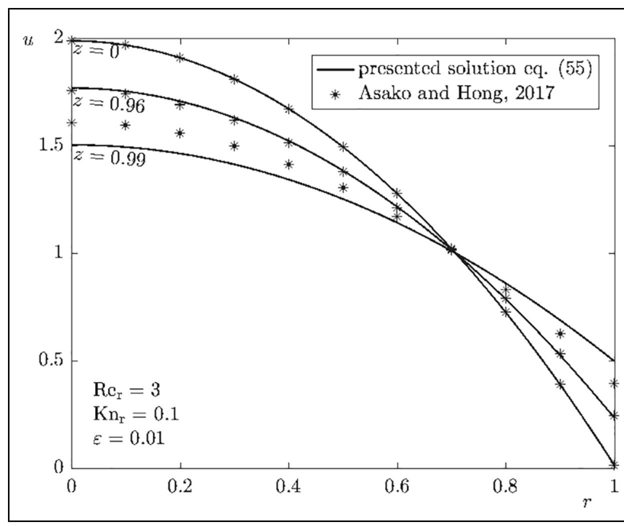

Figure 7. Velocity profiles at the different cross sections of the microtube for incompressible gas flow.

the microtube. Regardless of the miniature dimensions of the tube diameter and constant wall temperature, the presented model shows that the flow is non-isothermal.

The influence of rarefaction on the velocity field along the microtube is analyzed in Figure 4. It shows that, for rarefied gas flow, the slip velocity at the wall exists and increases along the microtube.

Next, we have considered the influence of $\mu(T)$ and $k(T)$ on pressure, temperature, and velocity field, for compressible and incompressible gas flow. In case of constant wall temperature, a minute temperature variation in microtube is obtained (Figure 3), so the effect of dynamic viscosity and thermal conductivity dependence on temperature is negligible. Therefore, the solution which does not comprise the influence of transport coefficient's dependence on temperature ($a = 0$) could be used. From the compressible gas flow solutions, by plugging in $a = 0$ into the equations (44) and (47), we get:

$$p = p_0 + \mathrm{Kn_r} p_1 = p_0 + \mathrm{Kn_r}\left[\frac{2-\sigma_v}{\sigma_v} 8\left(\frac{1}{p_0}-1\right) + 2\mathrm{Kn_r}\mathrm{Re_r^2}\frac{\ln p_0}{\pi p_0}\left(2 - \mathrm{Pr}\frac{\kappa-1}{\kappa}\right)\right] \tag{52}$$

$$\begin{aligned} u = u_0 + \mathrm{Kn_r} u_1 = {} & \frac{2}{p_0}\left(1-r^2\right) + \\ & + \mathrm{Kn_r}\left[\frac{2-\sigma_v}{\sigma_v}\frac{8}{p_0^2} + \frac{p_1{}'}{16\beta}\left(r^2-1\right)\right. \\ & \left. + \mathrm{Kn_r}\mathrm{Re_r^2}\frac{16}{\pi p_0^3}\left(\frac{r^6}{9} - \frac{r^4}{2} + r^2 - \frac{11}{18}\right)\right] \end{aligned} \tag{53}$$

Equation (46) for temperature solution remains in the same form.

For incompressible gas flow, solutions for pressure (48) and velocity (51) for $a = 0$ are reduced to:

$$p = p_0 + \mathrm{Kn_r} p_1 = p_0 - \frac{2-\sigma_v}{\sigma_v} 8\mathrm{Kn_r} \ln p_0 \tag{54}$$

$$\begin{aligned} u = u_0 + \mathrm{Kn_r} u_1 = {} & 2\left(1-r^2\right) \\ & + \mathrm{Kn_r}\left[\frac{2-\sigma_v}{\sigma_v}\frac{8}{p_0} + \frac{p_1{}'}{16\beta}\left(r^2-1\right)\right] \end{aligned} \tag{55}$$

while the temperature profile remains the same (50).

In Figures 5 to 7 solutions for pressure (54), temperature (50), and velocity distribution (55) in microtube for incompressible gas flow are presented. All pressure distributions presented in Figure 5 are obtained for the same $\mathrm{Re_r}$ number, that is, in this case

($a = 0$) for the same mass flow. It is shown that, for the same mass flow, rarefaction increase leads to the lower pressure in microtube.

In order to verify presented solutions, results for velocity (55) and temperature (50) are compared with Asako and Hong[20] results, which are obtained for incompressible thermally fully developed gas flow in microtube with constant wall temperature. For incompressible flow conditions, the model presented in this paper gives solution for thermally fully developed flow, that is, temperature profile does not change along the microtube. Comparing the presented results with temperature profile obtained by Asako and Hong,[20] which is fully developed at the exit, a good agreement is achieved, with relative error less than 1% (Figure 6). The velocity profile (55) in three cross sections of microtube is presented and compared with Asako and Hong[20] solution, resulting in a good agreement (Figure 7). Both solutions provide the increase of slip velocity at the wall, as well as the decrease of the maximum velocity, along the microtube.

Conclusions

Solutions for pressure, temperature, and velocity fields for stationary, axisymmetric, rarefied slip gas flow in microtube with constant wall temperature for moderately high values of Reynolds numbers are presented. Analytical solutions are obtained by macroscopic approach for compressible and incompressible gas flow.

Governing equations are analyzed for subsonic, slip gas flow with moderately high values of Reynolds number by assuming that the diameter of microtube is much smaller than its length and radial velocity is much smaller than longitudinal one. Velocity slip and temperature jump boundary conditions are incorporated into the presented model. Solution is obtained by perturbation method, that is temperature, pressure, density, longitudinal, and radial velocity are expressed in form of perturbation series. Two approximations are achieved, where the first one represents continuum flow conditions, while the second approximation represents the correction due to the slip and inertia effects.

Viscosity-temperature parameter a has an insignificant influence on temperature, pressure, and velocity fields. Hence, the simplified solutions obtained for $a = 0$ are also presented, both for compressible and incompressible gas flow. Temperature and velocity solutions for incompressible flow are compared with the results of Asako and Hong[20] and a good agreement is achieved.

Since the presented solutions are analytical, they are easy to use, they enable easy reproduction and can be exploited as accuracy validation of solutions attained in other ways, numerically or experimentally. The advantage of the presented solutions compared to results presented in open literature is that they simultaneously comprise several effects: rarefaction, compressibility, temperature field variability, inertia, and viscous dissipation. Moreover, the confirmation of accuracy of the applied perturbation method enables further research work on a number of other problems such as: flow through microtubes with a defined heat flux on the wall, flow between coaxial cylinders with the same or different wall temperatures and heat fluxes, etc.

Declaration of conflicting interests

The author(s) declared no potential conflicts of interest with respect to the research, authorship, and/or publication of this article.

Funding

The author(s) disclosed receipt of the following financial support for the research, authorship, and/or publication of this article: This work was supported by the Ministry of Education, Science and Technological Development, Republic of Serbia [contract number 451-03-9/2021-14/200105].

ORCID iD

Iva Guranov https://orcid.org/0000-0002-2411-389X

References

1. Gad-el-Hak M. *MEMS: introduction and fundamentals*. Boca Raton, FL: Taylor & Francis Group, 2006.
2. Karniadakis GE, Beskok A and Aluru N. *Microflows and nanoflows*. New York, NY: Springer-Verlag, 2005.
3. Sharipov FM and Seleznev VD. Rarefied gas flow through a long tube at any pressure ratio. *J Vac Sci Technol A* 1994; 12: 2933–2935.
4. Radenkovic D, Milicev S and Stevanovic N. Rarefied Gas flow in microtubes at low Reynolds numbers. *FME Trans* 2016; 44: 10–15.
5. Hemadri V, Biradar GS, Shah N, et al. Experimental study of heat transfer in rarefied gas flow in a circular tube with constant wall temperature. *Exp Therm Fluid Sci* 2018; 93: 326–333.
6. Xiao N, Elsnab J and Ameel T. Microtube gas flows with second-order slip flow and temperature jump boundary conditions. *Int J Therm Sci* 2009; 48: 243–251.
7. Spiga M and Vocale P. Slip flow in Elliptic microducts with constant heat flux. *Adv Mech Eng* 2012; 4: 481280.
8. Kushwaha HM and Sahu SK. Analysis of gaseous flow in a micropipe with second order velocity slip and temperature jump boundary conditions. *Heat Mass Transf* 2014; 50: 1649–1659.
9. Barışık M, Yazıcıoğlu AG, Çetin B, et al. Analytical solution of thermally developing microtube heat transfer including axial conduction, viscous dissipation, and rarefaction effects. *Int Commun Heat Mass Transf* 2015; 67: 81–88.

10. Aziz A and Niedbalski N. Thermally developing microtube gas flow with axial conduction and viscous dissipation. *Int J Therm Sci* 2011; 50: 332–340.
11. Chen S. Lattice Boltzmann method for slip flow heat transfer in circular microtubes: extended Graetz problem. *Appl Math Comput* 2010; 217: 3314–3320.
12. Cetin B and Bayer O. Evaluation of Nusselt number for a flow in a microtube using second-order slip model. *Therm Sci* 2011; 15: 103–109.
13. Maharjan D, Hadj-Nacer M, Ho MT, et al. Simulation of heat transfer across rarefied gas in annular and planar geometries: comparison of Navier-Stokes, S-Model and DSMC methods results. In: *ASME 2015 13th international conference on nanochannels, microchannels, and minichannels collocated with the ASME 2015 international technical conference and exhibition on packaging and integration of electronic and photonic microsystems*, San Francisco, CA, USA, 6–9 July 2015, paper no. ICNMM2015-48034, V001T04A032, pp.1–10.
14. Pantazis S and Valougeorgis D. Heat transfer through rarefied gases between coaxial cylindrical surfaces with arbitrary temperature difference. *Eur J Mech B Fluids* 2010; 29: 494–509.
15. Colin S. Gas microflows in the slip flow regime: a critical review on convective heat transfer. *J Heat Transf* 2012; 134: 020908.
16. Maxwell JC. On stresses in rarefied gases arising from inequalities of temperature. *Philos Trans R Soc London* 1879; 170: 231–256.
17. Smoluchowski von Smolan M. Ueber Wärmeleitung in verdünnten Gasen. *Ann Phys* 1898; 300: 101–130.
18. Stevanovic ND. A new analytical solution of microchannel gas flow. *J Micromech Microeng* 2007; 17: 1695–1702.
19. Milicev S and Stevanovic N. A microbearing gas flow with different walls' temperatures. *Therm Sci* 2012; 16: 119–132.
20. Asako Y and Hong C. On temperature jump condition for slip flow in a micro-channel with constant wall temperature. *J Heat Transf* 2017; 139: 072402.